Scientific paper

Bleaching Kinetic and Mechanism Study of Congo Red Catalyzed by ZrO_2 Nanoparticles Prepared by Using a Simple Precipitation Method

Hamid Reza Pouretedal[1,*] and Marzihe Hosseini[2]

[1] *Department of Chemistry, Malek-ashtar University of Technology, Shahin-shahr, Iran.*

[2] *Islamic Azad University, Shahreza branch, Shahreza, Iran*

** Corresponding author: E-mail: HR_POURETEDAL@mut-es.ac.ir. Tel: +98-312-591-2253, Fax: +98-312-522-0420*

Received: 10-11-2009

Abstract

Bleaching of Congo red catalyzed by ZrO_2 nanoparticles was study under UV and sunlight irradiations. The nanoparticles of ZrO_2 have been synthesized by controlled precipitation method. The concentration of $ZrOCl_2$ and ammonia reactants and the calcinations temperature of ZrO_2 were optimized for the control of nanoparticles size. Characterization of the prepared nanoparticles was studied by using XRD patterns, TEM images and FT-IR spectra. The tetragonal phase of zirconium oxide was obtained at 550 °C and show the most catalytic effect in dye degradation. The various parameters such as the irradiation time, amount of nanophotocatalyst, pH of samples, and initial concentration of Congo red were studied to find desired conditions of photodegradation process. The degradation 98% was achieved at pH 7 catalyzed by 0.7 g/L if ZrO_2 nanoparticles in duration time of 125 min. The effect of iso-PrOH, hydrogen peroxide and inorganic anions was studied on the degradation efficiency of dye. The degradation 98% was obtained in the presence of prepared nanosized zirconia in comparison with degradation 65% catalyzed by commercially zirconia.

Keywords: Photodegradation; Zirconia, Nanoparticles, Congo red, Photocatalyst.

1. Introduction

The major problem of colorants is the removal of dyes from eluents. In the textile industry, for example, ca. 100 billion gallons of waste water is discharged per annum into the waste water treatment systems. Untreated effluents may be highly colored and, thus, particularly objectionable if dis-charged into open waters. Their dye concentration may be well below 1 ppm. i.e. lower than any other chemicals found in waste water, but the dye will be visible even at such low concentrations.[1,2] Various methods have been used for removing organic compounds from waste water e.g. coagulation, denitrification, biodegradation, adsorption and different oxidation processes.[3–5] Azo dyes are the largest group of synthetic colorants known and the most common group released into the environment. Although they do not generally display extreme toxicity, azo dyes are an environmental problem because of their resistance to microbial degradation. However, in some cases, biodegradation can lead to reduction of the azo bond producing mutagenic and/or carcinogenic compounds.

The removal of the non-biodegradable organic chemicals is a crucial ecological problem. Dyes are important classes of synthetic organic compounds that used in the textile industry. They are common industrial pollutants. Due to the stability of modern dyes, conventional biological treatment methods for industrial wastewater are ineffective. Heterogeneous photocatalysis by semiconductor particles are a promising technology for the reduction of global environmental pollutants. Inorganic photocatalysts, such as TiO_2, ZnS, ZnO, CdS and Fe_2O_3 are shown a photocatalyst behavior for removing the organic pollutants.[6–9] Degradation of Congo red as azo dye was reported by several researchers. In these reports, TiO_2 as a famous semiconductor was used as photocatalyst.[10–12]

Nano-phase zirconia has been the focus of many researches because of its important applications such as oxygen sensor, solid state electrolytes for fuel cell and

gradient refractive index lenses. A number of wet chemical processes, such as homogeneous precipitation, sol-gel, micro-emulsion and high temperature hydrothermal process are known to produce nanocrystals of zirconia. However, the low temperature hydrolysis of zirconyl solution seemed to be an attractive approach due to the inexpensive starting material and process simplicity.[13–15]

ZrO_2, a widely used heterogeneous catalyst, is an *n*-type semiconductor with band-gap energy of 5.0 eV (reported values range between 3.25 and 5.1 eV depending on the preparation technique of the sample but the most frequent and accepted value is 5.0 eV) and conductance and valence band potentials of –1.0 and +4.0 V versus NHE, respectively, allowing its use as a photocatalyst in the production of hydrogen through water decomposition.[16] Although ZrO_2 presents an adsorption maximum around 250 nm, some samples show a non-negligible absorption in the near UV range (290–390 nm) and photocatalytic reactions could be performed under irradiation in this range; Litter and co-workers listed many ZrO_2-photocatalyzed reactions including production of hydrogen from water.[17,18] Photochemical reactions attract much attention as possible routes for harnessing solar energy but reports using natural sunlight are a few and preliminary.[19,20]

Here, we report the synthesis of ZrO_2 nanoparticles, characterization of prepared nanoparticles and bleaching kinetic and mechanism study of Congo red (CR) catalyzed by zirconia nanoparticles.

2. Experimental

2. 1. Synthesis of ZrO_2 nanoparticles

Zirconium oxychloride ($ZrOCl_2 \times 8H_2O$) and ammonia solution (25% w/w) with high purity and analytical grade were used as precursor for synthesis of ZrO_2 nanoparticles. A controlled precipitation procedure use to prepare the ZrO_2 nanoparticles.[13,14] The solutions were prepared in deionized and double distilled water. Firstly, 50 ml of 2.5 M ammonia solution was added to 50 ml of 0.1 M zirconium oxychloride solution drop by drop using a decanter while the mixture was stirred vigorously at room temperature (Fig. 1). The white $Zr(OH)_4$ precipitates in time of addition of precipitant agent. The precipitated nanoparticles of $Zr(OH)_4$ were then centrifuged at 3000–4000 rpm, washed with water and ethanol several times. The $Zr(OH)_4$ nanoparticles were heated in an autoclave in temperature of 50–100 °C for about 4–16 h. Finally, the white ZrO_2 powders were calcinated in an oven in temperature of 200–750 °C for about 3–6 h and then stored for further use.

2. 2. Characterization of ZrO_2 Nanoparticles

The prepared nanoparticles characterize by using XRD patterns, IR spectra, TG/DTG analysis and TEM images. An X-ray Diffractometer Bruker D8ADVANCE Germany with anode of Cu, wavelength: 1.5406 Å (Cu Kα) and filter of Ni apply to record the X-ray diffraction (XRD) patterns of nanosized zirconia. The nanoparticles size was estimated by a JEOL JEM-1200EXII transmission electron microscope (TEM) operating at 120 kV. The supporting grids were formvar-covered, carbon-coated, 200-mesh copper grids. IR-spectra of ZrO_2 nanoparticles in range 4000–400 cm^{-1} was recorded by using Nicolet Impact 400D FT-IR Spectrophotometer. B.E.T (Brunauer-Emmett-Teller) surface area of nanoparticles was determined by using Monosorb Quantochorom.

2. 3. Bleaching of Congo Red

The kinetic and mechanism of Congo red ($C_{32}H_{22}N_6Na_2O_6S_2$) bleaching were studied in the presence of ZrO_2 nanoparticles as photocatalyst.

A photocatalytic reactor system with a mercury low pressure lamp (70 W) with λ_{max} = 332 nm and light intensity 22 W/m^2 uses to measure degradation of CR. The lamp and the tube were then immersed in the photoreactor cell with a light path of 3.0 cm. The photoreactor was fil-

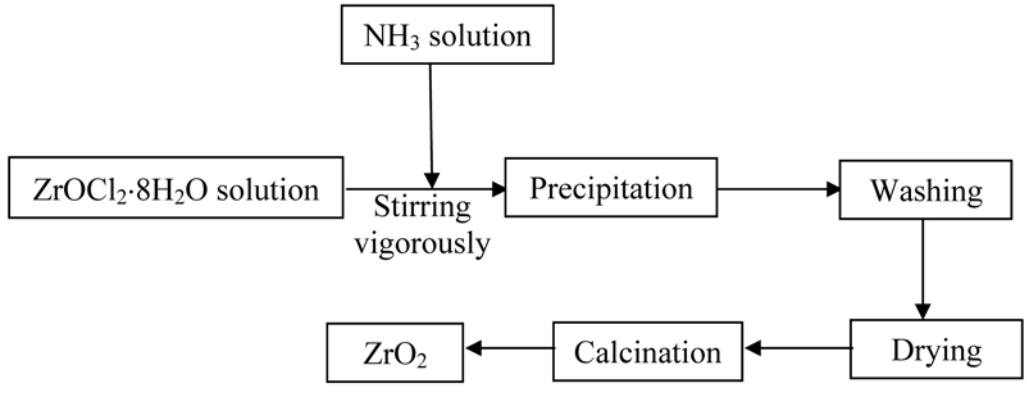

Figure 1: Flow diagram of ZrO_2 preparation

led with 50 ml sample contain 10.0–50.0 mg/L CR and 0.0–1.0 g/L ZrO_2 nanoparticles The temperature of photoreactor was kept at 25 °C with a water-cooled jacket on its outside. A magnetic stirrer applies to ensure that the suspension of the heterogeneous catalyst is uniform during the degradation. The samples were collected at regular intervals, filtered through Millipore membrane filters, and centrifuged to remove the nanocatalyst. The collected samples were analyzed to measure the absorbance of dye by using a UV-Vis spectrophotometer Carry-100.

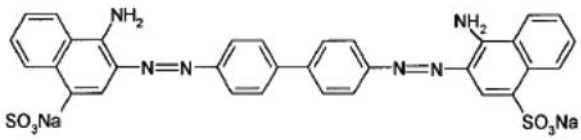

Congo red

The decrease of absorbance value of samples at λ_{max} of dye (510 nm) after irradiation in a certain time intervals shows the rate of decolorization efficiency (%D) and calculated by Eq(1):

$$\%D = 100 \times [(C_o - C_t)/C_o] = 100 \times [(A_o - A_t)/A_o] \quad (1)$$

In Eq (1), C_o and C_t are the initial concentration and concentration of dye at time t, respectively, and A_o and A_t are the initial absorbance and absorbance of dye at time t, respectively.

2. 4. Kinetic Study and Mechanism of Dye Bleaching

The simplified pseudo-first order kinetic model of Langmuir–Hinshelwood (Eq 2) use to calculate the apparent rate constant of degradation process catalyzed by 0.7 g/L of ZrO_2 nanoparticles at initial concentrations 10, 20, 30, 40 and 50 ppm of CR at pH 7.

$$\ln(C_o/C_t) = kKt = K_{app}t \quad (2)$$

In Eq(2), C is concentration of the dye (mg/L), t is irradiation time (min), k is reaction rate constant (min^{-1}), K is the adsorption coefficient of the dye onto the photocatalyst particles (L/mg) and k_{app} is the apparent rate constant (min^{-1}).

The effect of H_2O_2 and isopropanol was investigated to foresight the degradation mechanism of azo-dye. Also, the CR bleaching catalyzed by nanosized zirconia was studied in the presence chloride, bicarbonate, sulfate, chlorate, nitrate and persulfate anions. The hydrogen proxide (25% w/w) and salts of NaCl, Na_2SO_4, $NaHCO_3$, $NaClO_3$ and $NaNO_3$ and $Na_2S_2O_8$ were analytical reagent grade quality and isopropanol was HPLC grade quality.

3. Results and Discussion

3. 1. Characterization of ZrO_2 Nanoparticles

Figs. 2A-2C show the diffraction pattern of the ZrO_2 nanoparticles treated at 250, 550 and 750 °C, respectively. The amorphous phase was observed at calcinations temperature of 250 °C. Whereas, the crystalline forms of tetragonal were seen at temperatures 550 and 750 °C. The tetragonal phase is dominant for zirconium oxide at 550 °C, but, the percentage of monoclinic phase is increased with increasing of temperature (Fig. 2C). Tetragonal phase was characterized by peaks located at 30, 51 and 61° (2θ).[21] This zirconia phase has been reported to be the most active.[14,15] To obtain this phase at temperatures below of 1200 °C is an advantage of proposed synthesis method. The average tetragonal (D_T) crystallite sizes were calculated 3 and 4 nm from the $(1\ 1\ 1)_T$ diffraction peak using Scherrer's equation (Eq. 3) for ZrO_2 calcinated at 550 and 750 °C, respectively.[22]

$$D_T = (0.9\lambda)/(\beta \cos \theta) \quad (3)$$

In Eq. 3, D is the average crystallite size in nm, λ is the radiation wavelength (0.154 nm), β is the corrected half-width at half-intensity and θ is the diffraction peak angle.

Fig. 3 shows FT-IR spectra of the zirconia powder at temperature of 550 °C. The bands at 3443 cm^{-1} and 1630 cm^{-1} correspond to the vibration of stretching and deformation of the O–H bond due to the absorption of water and coordination water, respectively. Another important absorption band at 461 cm^{-1} is related to the vibration of the Zr–O bond in ZrO_2.[23]

The TEM images of ZrO_2 treated at 550 °C were shown in Figs. 4A and 4B. It is seen that the ZrO_2 is composed of some agglomerated particles with an average size of less than 50 nm. The TEM analysis also shows the nanoparticles are sintered together and most of the nanoparticles have a slightly irregular, rounded shape.

3. 2. Photodegradation of Congo Red

Degradation efficiency of CR versus time catalyzed by ZrO_2 nanoparticles (0.0–1.0 g/L) was shown in Fig. 5. The model is developed by following the photocatalytic mechanism, which is well understood and reported.[24] The positive holes and electrons generated by UV on photocatalyst, involve in the formation of the hydroxyl radicals. The reaction between the positive holes and the adsorbed water forms hydroxyl species. The dye degrades by the attack of direct hole and hydroxyl species. The radical hydroxyl with $E^o = +3.06$ V is a strong oxidative and oxidize dyes as non-selective to mineral species as partial or complete.[24] ZrO_2, a widely used heterogeneous catalyst, is an *n*-type semiconductor with band gap energy of 5.0 eV.[16] The other reported values are between 3.25 and 5.1 eV depending on the preparation technique of the sample.[16]

The conductance and valence band potentials of –1.0 and +4.0 V versus NHE, respectively, allowing its use as a photocatalyst in the photocatalytic reactions. Although ZrO_2 presents an adsorption maximum around 250 nm, some samples show a non-negligible absorption in the near UV range (290–390 nm) and photocatalytic reactions could be performed under irradiation in this range.[25]

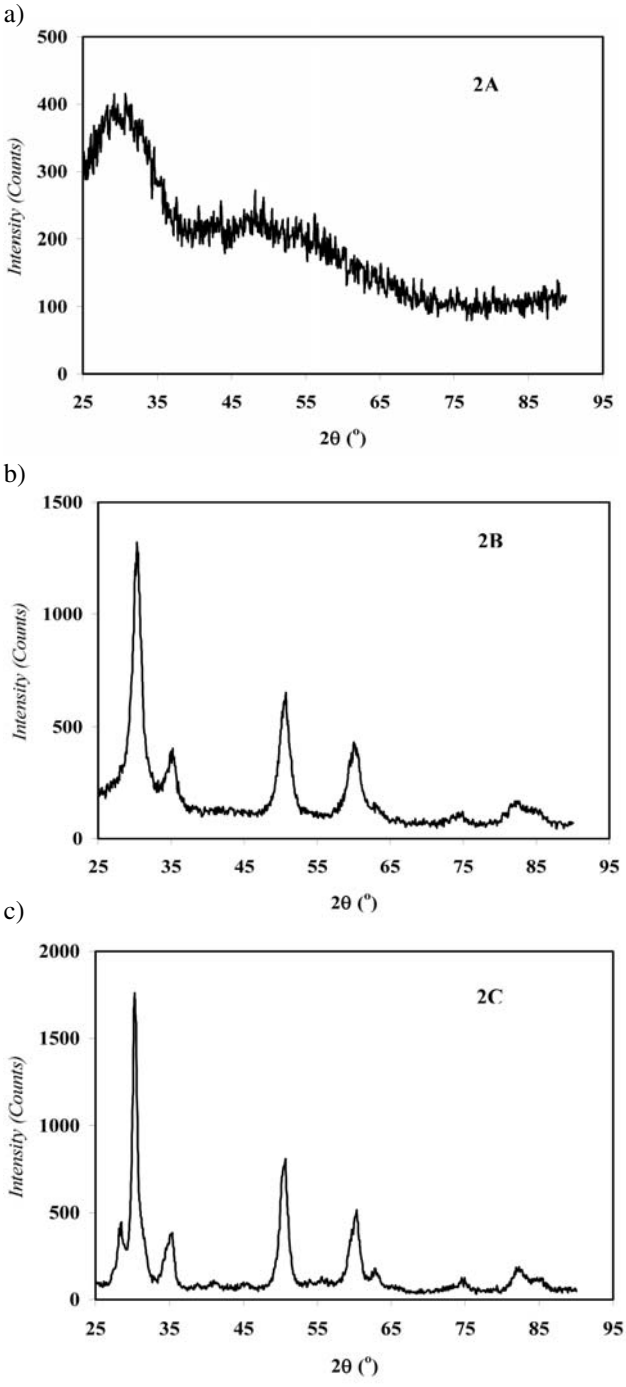

Figures 2a), b) and c). XRD pattern of ZrO_2 nanoparticles treated at 250, 550 and 750 °C, respectively.

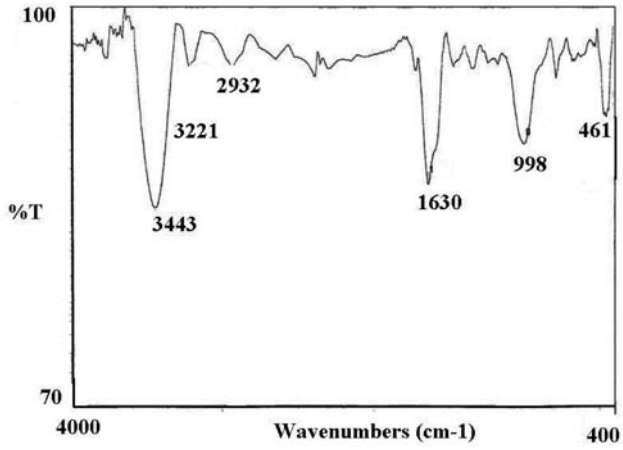

Figure 3. IR spectra of ZrO_2 nanoparticles treated at 550 °C.

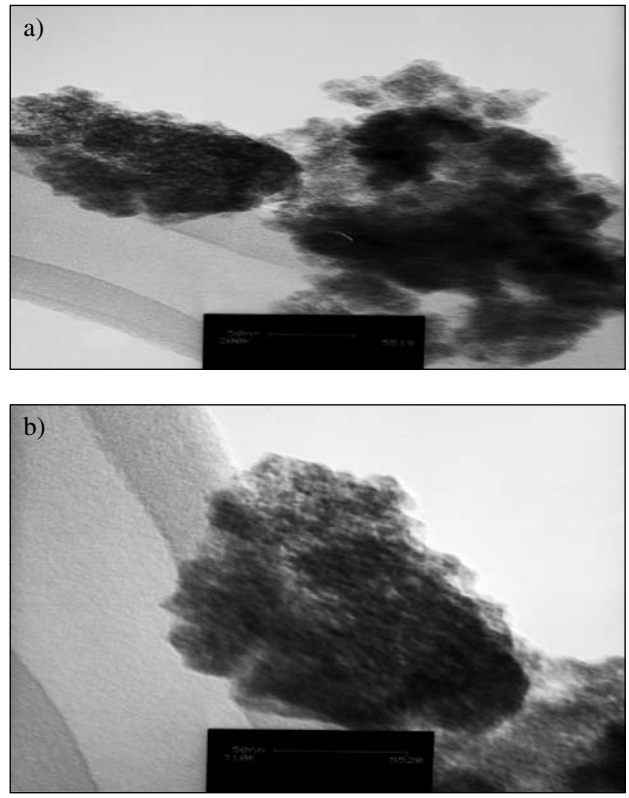

Figures 4a) and b). TEM images of ZrO_2 nanoparticles treated at 550 °C.

The results in Fig. 5 also show the photodegradation efficiency of dye was increased with increasing the amount of photocatalyst from 0.2 to 0.7 g/L. Degradation efficiency diminish with loading of photocatalyst above of 0.7 g/L. It is noticed to the total active surface area and availability was increased with the increasing of photocatalyst dosage. However, as the loading was increased beyond the optimum amount, due to an increase in turbidity of the suspension with high dose of photocatalyst, there

will be decrease in penetration of UV light and photoactivated volume of suspension. In these conditions, the penetration depth of the photons is decreased and less catalyst nanoparticles could be activated.[26,27] Hence, the optimum dosage of photocatalyst for degradation of Congo red is to be found 0.7 g/L.

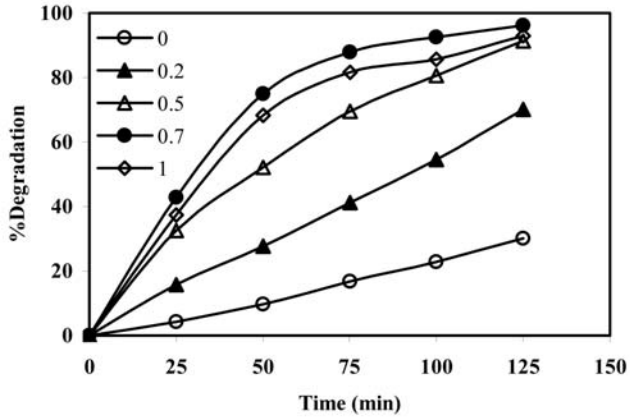

Figure 5. Degradation efficiency of Congo red versus time in different dosages (g/L) of ZrO_2 nanoparticles.

The role of pH on degradation of pollutants catalyzed by heterogeneous photocatalyst is important because the surface charge as well as isoelectric point is pH dependent. As the other hand the pH of samples also influence on the dye molecules charge. Fig. 6 shows results of Congo red photodegradation in pH range of 3.0–11.0 in the presence of 0.7 g/L ZrO_2 nanocatalyst. The HCl and NaOH solutions with concentrations of 1.0×10^{-2} M were used for adjustment of solutions pH. The degradation efficiency was increased with increasing the pH from 3 to 7 and then decreased at higher pHs. Although, degradation yield is comparable in pH 3–7, however, the most degradation was obtained at pH 7. There are several factors that influence on the pH effects in the photocatalytic degradation process of dyes. First, it is related to the acid-base property of the metal oxide surface and can be explained on the basis of zero point charge. The isoelectric points (IEP) of metal oxide ceramics are used extensively in material science in various aqueous processing steps (synthesis, modification, etc.). For these surfaces, present as colloids or larger particles in aqueous solution, the surface is generally assumed to be covered with surface hydroxyl species, M–OH (where M is a metal such as Al, Si, etc.). At pH values above the IEP, the predominate surface species is M–O, while at pH values below the IEP, $M–OH_2^+$ species predominate.[28]

The isoelectric point of pure ZrO_2 is at pH 4–7 and thus the surface of zirconia particles is negative in pH > 7 and positive in pH < 4.[29] As the other hand, the Congo

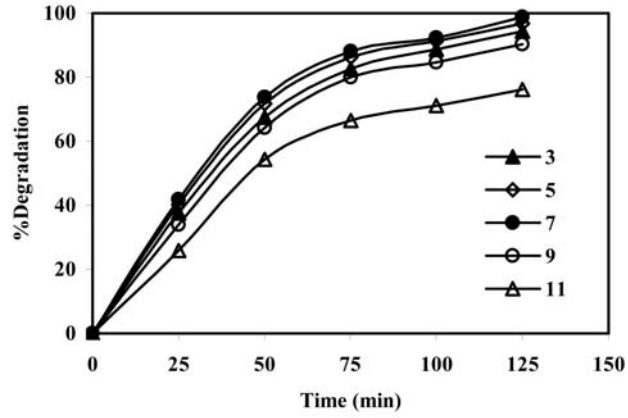

Figure 6. The Effect of pH on the degradation efficiency of Congo red catalyzed by 0.7 g/L ZrO_2 nanoparticles.

red molecules have the negative charge in basic pHs due to sulfonic group. Thus, it is not surprising the increasing repulsion forces between dye molecules and ZrO_2 nanoparticles in pH > 7. Therefore, as seen from Fig. 6 the degradation efficiency decreases in alkaline samples.

The degradation of Congo red was studied at different initial concentrations in the range of 10.0–50.0 mg/L (Fig. 7). As seen from Fig. 7, the rate of degradation decreases with increasing the initial concentration of dye. Apparently, in high concentrations of Congo red, more dye molecules were adsorbed on the surface of the catalyst and thus the generation of hydroxyl radicals at the catalyst surface was reduced since the active sites were occupied by dye molecules. Moreover, as the concentration of dye increased, this also caused the dye molecules to adsorb light with the result that fewer photons could reach the photocatalyst surface and so, photodegradation efficiency decreased.[5,30]

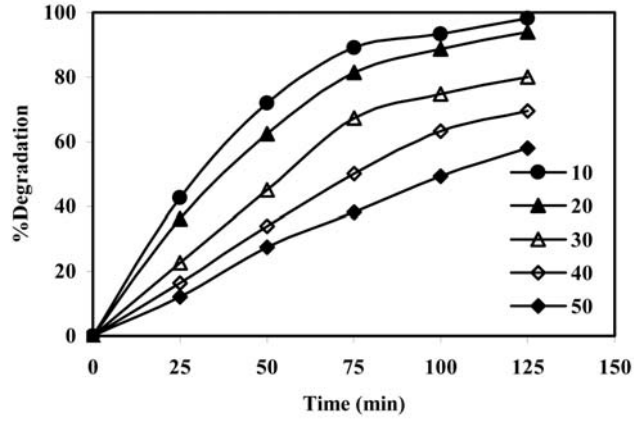

Figure 7. The Effect of initial concentration of Congo red (mg/L) on the degradation efficiency in the presence of 0.7 g/L ZrO_2 nanoparticles.

3. 3. Kinetic Rate Constants

Langmuir–Hinshelwood expression (Eq. 4) can be used for study the effect of initial concentration of dye pollutants on the rate of photocatalytic degradation.[31]

$$r = \frac{k_1 k_2 C_o}{1 + k_1 C_o} \quad (4)$$

Where k_1, k_2 and C_o are adsorption constant, specific rate constant and initial concentration of the dye, respectively. The apparent rate constant value obtained at low initial dye concentrations by the product of k_1 and k_2. The Eq. (5) is obtained by integration Eq. (4).

$$t = \frac{1}{k_1 k_2} \ln \frac{C_o}{C} + \frac{1}{k_2}(C_o - C) \quad (5)$$

Where t is the time (min) required for decreasing the initial concentration (C_o) of the dye to concentration at time t (C). Since the dye concentration is very low, the second term of the expression becomes small when compared with the first one and under these conditions the Eq. (5) reduces to Eq. (6).

$$t = \frac{1}{k_1 k_2} \ln \frac{C_o}{C} + \frac{1}{k_2}(C_o - C) \quad (6)$$

This kinetic model was applied to the experimental data and apparent rate constants (k_{app}) of degradation at different initial concentrations of CR (Fig. 7) were obtained from the plots slope of ln(C_o/C) versus time. The plots are shown in Fig. 8 and the apparent rate constants are given in Table 1.

Table 1: The apparent rate constants of Congo red degradation.

[CR], mg/L	K_{app}, min^{-1}
10	31.110^{-3}
20	19.410^{-3}
30	13.710^{-3}
40	9.910^{-3}
50	7.210^{-3}

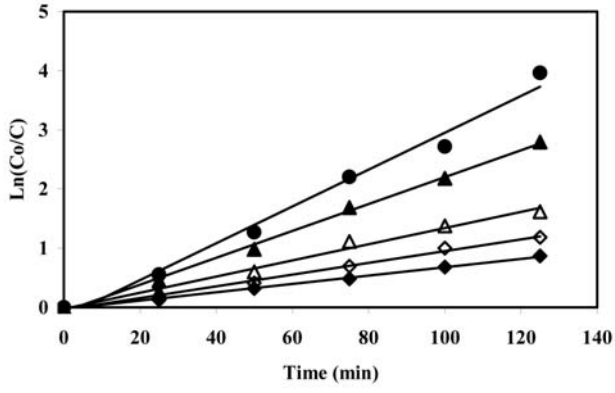

Figure 8. The plot of ln(Co/C) versus time at different initial concentrations of Congo red accordance with Fig. 7.

The half-life of dye degradation at various initial concentrations was raised from Eq. (7).

$$t_{0.5} = \frac{C_o}{2k_2} + \frac{0.693}{k_1 k_2} \quad (7)$$

Plot of $t_{0.5}$ versus C_o is indicated in Fig. 9. The k_1 and k_2 values are obtained 4.071 L/mg and 0.277 mg/L.min from slope and intercept of plot, respectively.

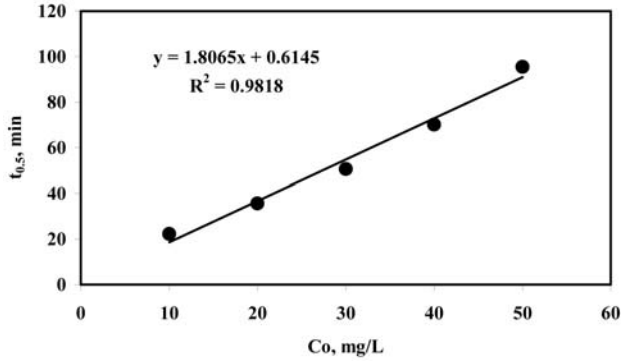

Figure 9. The plot of $t_{0.5}$ versus initial concentrations of Congo red.

3. 4. The Role of Primary Active Species

The effect of iso-PrOH as a scavenger was studied to estimate the oxidation mechanism of CR. As seen from Fig. 10, the degradation yield of CR was decreased with increasing of %V/V iso-PrOH. Isopropanol (*i*-PrOH) as a good scavenger is more easily oxidized by $OH^{\bullet}$ radicals with rate constant of reaction 1.9×10^9 M^{-1} s^{-1}.[32,33] The apparent rate constant of CR degradation reduce to 8.7×10^{-3} min^{-1} in the presence of 6% V/V of iso-PrOH. The reduction of k_{app} of CR indicates the $OH^{\bullet}$ radicals played a considerable role in the photoreaction of CR degradation.

Alcohols such as MeOH, EtOH and iso-PrOH are usually used as diagnostic tools of $OH^{\bullet}$ radicals mediated mechanism. Small amounts of ethanol as a scavenger inhibited the photocatalytic degradation of azo dyes of Acid Red 14, AR14 and AO7 on ZnO and TiO_2, respectively.[34] Thus, it can be concluded that $OH^{\bullet}$ radicals played a major role in photodegradation of azo dyes catalyzed by a semiconductor.

Experiments were done to study the effect of H_2O_2 on the photodegradation yield of CR. As seen from Fig. 11, degradation efficiency increases as the concentration of hydrogen peroxide increases up to 0.5 mM and then decreased in higher concentrations of H_2O_2. The concentration of $OH^{\bullet}$ radical can be increased in the presence of H_2O_2 because it inhibit the electron–hole recombination according to the Eq. (8).

$$ZrO_2(e^-) + H_2O_2 \rightarrow ZrO2 + OH^- + OH^\bullet \quad (8)$$

There are two functions for hydrogen peroxide in the photocatalytic degradation.[35] Electrons in conduction band can be adsorbed by H_2O_2 and thus the charge separation promoted in semiconductor. Also, it forms hydroxyl radical (Eq. 9 and 10).

$$H_2O_2 + e^- \rightarrow OH^- + OH^\bullet \quad (9)$$

$$H_2O_2 + O_2^{-\bullet} \rightarrow OH^- + OH^\bullet + O_2 \quad (10)$$

With respect to equations of (9) and (10) and increasing of $OH^\bullet$, it is expected to increase the rate of photocatalytic reactions. An increasing 30% in apparent rate constant of CR degradation (20 mg/L) was seen in the presence of 0.5 mM H_2O_2 (25.2×10^{-3} in comparison to 19.4×10^{-3}). The reduction in degradation efficiency was observed after the quantum level of H_2O_2. The inhabitation effect of a high concentration of H_2O_2 can be due adsorption of it on the catalyst surface. In this conditions, the hydrogen peroxide molecules act as $^\bullet OH$ radicals and hole scavengers (Eqs. 11, 12 and 13).[36]

$$H_2O_2 + {}^\bullet OH \rightarrow H_2O + HO_2^\bullet \quad (11)$$

$$HO_2^\bullet + {}^\bullet OH \rightarrow H_2O + O_2 \quad (12)$$

$$H_2O_2 + h_{vb}^+ \rightarrow HO_2^\bullet + H^+ \quad (13)$$

Reduction of k_{app} in higher concentration of H_2O_2 show that the $^\bullet OH_2$ formed is significantly less reactive than the $^\bullet OH$. As the other hand, reaction of holes with H_2O_2 is due to inhibit the generation of $^\bullet OH$ radicals and thereby decrease the degradation rate.

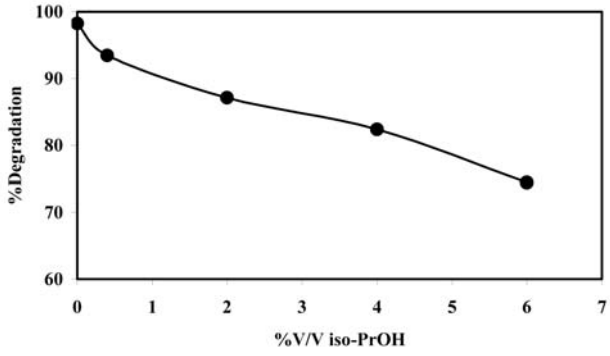

Figure 10. The Effect of iso-PrOH initial concentration on the degradation efficiency of Congo red (10 mg/L) catalyzed by 0.7 g/L ZrO_2 nanoparticles in duration time 125 min.

3. 5. The Effect of Anions on Photocatalytic Degradation

The actual wastewater of dyestuff often contains many other chemical materials such as many co-existing negative ions. The influence of chloride, bicarbonate, sulfate, chlorate, nitrate, and persulfate anions from their sodium salts (500 mg/L) was investigated on the CR degradation. The results were shown in Fig. 12. It is seen from Fig. 12, the anions Cl^-, HCO_3^-, SO_4^{2-} and NO_3^- show an inhibitory effect on the CR photodegradation. Their negative effect are in the following order $HCO_3^- > Cl^- > SO_4^{2-} > NO_3^-$. The active sites on the surface of the catalyst are blocked by these anions and therefore the reactivity of the photocatalyst is decreased. The bicarbonate anion with p-H > 7 shows the inhibitory effect (Fig. 6). Also, anionic species can behave as hole (h^+) and $^\bullet OH$ scavengers and thus the color removal is prolonged. The inorganic radical anions such as $Cl^\bullet$, $NO_3^\bullet$, $SO_4^{-\bullet}$ and $HCO_3^\bullet$ are formed under these circumstances.[37, 38] Although these radicals show activity but are not as reactive h^+ and $^\bullet OH$ and thus the observed retardation effect still thought to be the strong adsorption of the anions on the ZrO_2 surface. However, the degradation efficiency of CR is increased in the presence of $S_2O_8^{2-}$ and ClO_3^- in duration time of 75 min in order $S_2O_8^{2-} > ClO_3^-$. The observed positive effect of is due to oxidative activity of these anions. Thus, the photodegradation yield is increased due to increasing of photogenerated electrons.[39]

3. 6. Photoreativity of Nanosized Zirconia Under Sunlight Irradiation

The photodegradation of CR was studied under sunlight irradiation catalyzed by nanosized ZrO_2. The apparent rate constant was obtained 18.6×10^{-3} min^{-1} for degradation 10 ppm dye in the presence of 0.7 g/L catalyst. The degradation 97% was resulted in time 125 min. Comparison k_{app} photodegradation CR under UV and sunlight irradiations indicate a considerable activity for synthesized nanoparticles.

Also, the catalytic activity of prepared nanoparticles is compared to commercially ZrO_2 with analytical purity (Merck). The specifics and results are collected in Table 2. B.E.T (Brunauer-Emmett-Teller) surface area of prepared nanoparticles was determined by using Monosorb Quan-

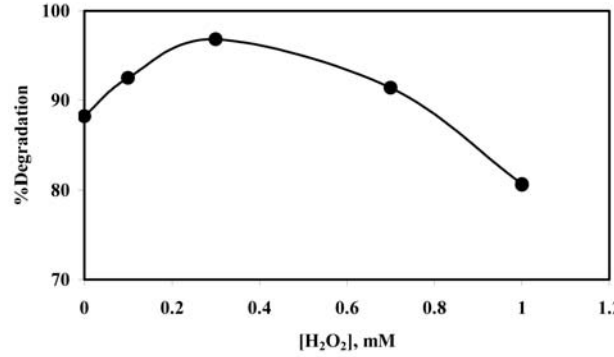

Figure 11. The Effect of hydrogen peroxide concentration on the degradation efficiency of Congo red (10 mg/L) catalyzed by 0.7 g/L ZrO_2 nanoparticles in duration time 75 min.

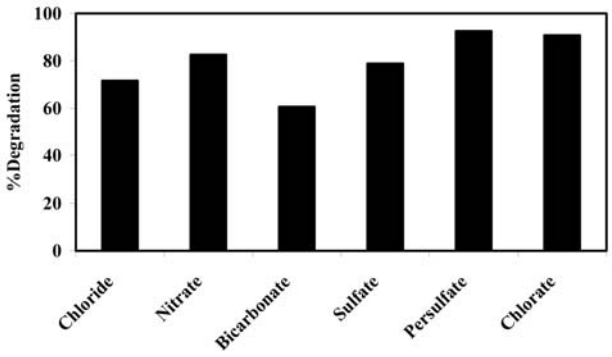

Figure 12. The Effect of negative ions concentration on the degradation efficiency of Congo red (10 mg/L) catalyzed by 0.7 g/L ZrO_2 nanoparticles in duration time 75 min.

tochorom and obtained 250 m^2/g. The degradation efficiency 98 and 65% for dye degradation catalyzed by prepared nanosized zirconia and commercially zirconia, respectively, indicating prominent activity for synthesized ZrO_2 nanoparticles. The usability of zirconia was study in 4-cycles under sunlight irradiation. After each cycle, the catalyst is removed from sample, washed with water and ethanol and treated at 250 °C in duration 2 h. Photocatalytic activity reproducibility of prepared nanoparticles was proved with dye degradation of 98–92% in four-cycles. While, a decrease 33% in degradation yield of CR was seen after 4-times use from commercially ZrO_2.

4. Conclusion

The ZrO_2 nanoparticles can be prepared by a simple precipitation method in the absence of any capping agent. The prepared nanoparticles show a photocatalytic activity in photodegradation process of a dye pollutant in a kinetic pseudo first-order reaction. The photocatalytic activity of zirconia decrease in the presence of iso-PrOH and thus the hydroxyl radicals played a major role in photodegradation of Congo red. The presence 0.5 mM H_2O_2 increase the apparent rate constant from 19.4×10^{-3} to 25.2×10^{-3} min^{-1}.

Table 2: Some characteristic properties of synthesized nano–ZrO_2 and commercially ZrO_2 and the results of CR photodegradation.

Property	Synthesized Nano-ZrO_2	Commercially ZrO_2
Crystalline type	Tetragonal	Tetragonal
Crystallite size	< 50 nm	> 15 m
ZrO_2 content (%)	> 99%	>98.5%
BET surface area (m^2 g^{-1})	250	50
%Degradation CR in time 125 min under sunlight	>98%	65%
Reusability	4-cycles with %D=98–92%	4–cycles with %D=65–32%

5. References

1. R. Molinari, F. Pirillo, M. Falco, V. Loddo, L. Palmisano, *Chem. Eng. Process.* **2004**, *43*, 1103–1114.
2. K. I. Konstantinou, A. A. Triantafyllos, *Appl. Catal. B* **2004**, *49*, 1–14.
3. S. Bilgi, C. Demir, *Dyes Pigments* **2005**, *66*, 69–76.
4. N. Guetta, H. A. Amar, *Desalination* **2005**, *185*, 427–437.
5. A. Mills, A. Belghazi, R. H. Davies, D. Worsley, S. Morris, *J. Photochem. Photobiol. A* **1994**, *79*, 131–139.
6. M. Vautier, C. Guillard, J. M. Herrmann, *J. Catal.* **2001**, *201*, 46–59.
7. H. R. Pouretedal, H. Eskandari, M. H. Keshavarz, A. Semnani, *Acta Chim. Slov.* **2009**, *56*, 353–361.
8. H. R. Pouretedal, A. Norozi, M. H. Keshavarz, A. Semnani, *J. Hazard. Mater.* **2009**, *162*, 674–681.
9. M. A. Behnajady, N. Modirshahla, R. Hamzavi, *J. Hazard. Mater. B* **2006**, *133*, 226–232.
10. K. Melghit, S. S. Al-Rabaniah, *J. Photochem. Photobiol. A* **2006**, *184*, 331–334.
11. K. Rajeshwar, M. E. Osugi, W. Chanmanee, C. R. Chenthamarakshan, M. V. B. Zanoni, P. Kajitvichyanukul, R. Krishnan-Ayer, *J. Photochem. Photobiol. C* **2008**, *9*, 171–192.
12. M. N. Chong, B. Jin, C. W. K. Chow, C. P. Saint, *Chem. Eng. J.* **2009**, *152*, 158–166.
13. K. L. Chen, A. S. T. Chiang, H. K. Tsao, *J. Nanopart. Res.* **2001**, *3*, 119–126.
14. M. Rezaei, S. M. Alavi, S. Sahebdelfar, L. Xinmei, Z. F. Yan, *J. Mater. Sci.* **2007**, *42*, 7086–7092.
15. M. Rezaei, S. M. Alavi, S. Sahebdelfar, Zi-Feng Yan, H. Teunissen, J. H. Jacobsen, J. Sehested, *J. Mater. Sci.* **2007**, *42*, 1228–1237.
16. C. Karunakaran, S. Senthilvelan, *J. Mol. Catal. A* **2005**, *233*, 1–8.
17. Y. Xu, M. A. A. Schoonen, *Am. Mineral.* **2000**, *85*, 543–556.
18. S. G. Botta, J. A. Navio, M. C. Hidalgo, G. M. Restrepo, M. I. Litter, *J. Photochem. Photobiol. A* **1999**, *129*, 89–99.
19. G. Alhakimi, L. H. Studnicki, M. Al-Ghazali, *J. Photochem. Photobiol. A* **2003**, *154*, 219–228.
20. C. Karapire, H. Kolancilar, U. Oyman, S. Icli, *J. Photochem. Photobiol. A* **2002**, *153*, 173–184.
21. M. N. Tahir, L. Gorgishvili, J. Li, T. Gorelik, U. Kolb, L. Nasdala, W. Tremel, *Solid State Sci.* **2007**, *9*, 1105–1109.
22. H. P. Klug, L. E. Alexander, X-Ray Diffraction Methods for Polycrystalline and Amorphous Materials, John Wiley and Sons, New York, **1954**.
23. V. Santos, M. Zeni, C. P. Bergmann, J. M. Hohemberger, *Rev. Adv. Mater. Sci.* **2008**, *17*, 62–70.
24. M. R. Hoffmann, S. T. Martin, W. Choi, D. W. Bahnemannt, *Chem. Rev.* **1995**, *95*, 69–96.
25. M. Alvarez, T. López, J. A. Odriozola, M. A. Centeno, M. I. Domínguez, M. Montes, P. Quintana, D. H. Aguilar, R. D. González, *Appl. Catal. B* **2007**, *73*, 34–41.
26. R. K. Wahi, W. W. Yu, Y. Liu, M. L. Mejia, J. C. Falkner, W. Nolte, V. L. Colvin, *J. Mol. Catal. A* **2005**, *242*, 48–56.

27. K. Dai, H. Chen, T. Peng, D. Ke, H. Yi, *Chemosphere* **2007**, *69*, 1361–1367.
28. J. Sun, Y. Wang, R. Sun, S. Dong, *Mater. Chem. Phys.* **2009**, *115*, 303–308.
29. J. W. Moon, H. L. Lee, J. D. Kim, G. D. Kim, D. A. Lee, H. W. Lee, **1999**, *38*, 214–220.
30. A. N. Rao, B. Sivasankar, V. Sadasivam, *J. Mol. Catal. A* **2009**, *306*, 77–81.
31. R. W. Matthews, *J. Phys. Chem.* **1987**, 91, 3328–3333.
32. Y. Chen, S. Yang, K. Wang, L. Lou, *J. Photochem. Photobiol. A* **2005**, *172*, 47–54.
33. P. Calza, E. Pelizzetti, *Pure Appl. Chem.* **2001**, *73*, 1839–1848.
34. N. Daneshvar, D. Salari, A. R. Khataee, *J. Photochem. Photobiol. A* **2004**, *162*, 317–322.
35. N. Daneshvar, S. Aber, M. S. Seyed Dorraji, A. R. Khataee, M. H. Rasoulifard, *Int. J. Chem. Biomol. Eng.* **2008**, *4*, 24–29.
36. S. K. Kansal, M. Singh, D. Sud, *J. Hazard. Mater.* **2007**, *141*, 581–590.
37. N. Sobana, M. Swaminathan, *Sep. Purif. Technol.* **2007**, *56*, 101–10.
38. K. Wang, J. Zhang, L. Lou, S. Yang, Y. Chen, *J. Photochem. Photobiol. A* **2004**, *165*, 201–207.
39. C. C. Chen, C. S. Lu, Y. C. Chung, J. L. Jan, *J. Hazard. Mater.* **2007**, *141*, 520–528.

Povzetek

Sintetizirali smo nanodelce ZrO_2 ter jih okarakterizirali z rentgensko difrakcijo (XRD), FT-IR spektroskopijo ter elektronsko mikroskopijo (TEM). Pri 550 °C smo ZrO_2 določili tetragonalno strukturo. Nanodelce ZrO_2 smo uporabili kot katalizator v raziskavah degradacije barvila kongo rdeče z obsevanjem z UV in s sončno svetlobo. Pri eksperimentu smo spreminjali čas obsevanja, pH vzorca, začetno koncentracijo barvila ter maso katalizatorja. Pri pH vrednosti 7, koncentraciji barvila 0.7 g/L in času obsevanja 125 min smo ugotovili 98 % razpad barvila. Dodatno smo proučevali tudi vpliv izopropanola, vodikovega peroksida in različnih anorganskih ionov na razgradnjo barvila.